

Electrochemical Behavior of Iron and Magnesium in Ionic Liquids

Lucas Lodovico,[†] Vitor L. Martins,[†] Tânia M. Benedetti and Roberto M. Torresi*

Instituto de Química, Universidade de São Paulo (USP), CP 26077, 05513-970 São Paulo-SP, Brazil

Neste trabalho, foi estudado o comportamento eletroquímico de Mg e Fe em líquidos iônicos (ILs). Para melhorar o entendimento do comportamento de Mg em IL baseado no ânion bis(trifluorometanosulfonamida) ([Tf₂N]), nós realizamos uma série de experimentos de voltametria cíclica. Os resultados mostraram deposição/dissolução de Mg irreversível em alta concentração de água (ca. 1300 ppm, 50 mmol L⁻¹) e uma reversibilidade muito baixa (7.3%) em uma concentração moderada de água (ca. 65 ppm, 5 mmol L⁻¹). A formação de um filme na superfície do eletrodo e a presença de Mg foi confirmada por microscopia eletrônica de varredura-espectrometria de energia dispersiva de raios-x (MEV-EDS). A irreversibilidade do processo indica a formação de um filme passivante. Como a presença de água impacta a reversibilidade do processo, foram realizados estudos de deposição/dissolução de Fe utilizando microeletrodos para avaliar como a água modifica a reversibilidade do processo e a difusão dos íons utilizando dois IL diferentes. A água tem um papel importante na reversibilidade da deposição/dissolução de Fe sendo a reação menos reversível na mistura seca. A difusão do íon de Fe também é modificada, já que a esfera de coordenação do íon Fe tem um grande impacto na presença e ausência de água, mas isto depende da habilidade de coordenação do cátion do IL.

In this work, the electrochemical behavior of Mg and Fe in ionic liquids (IL) were studied. We performed a series of cyclic voltammetry experiments to improve the understanding of Mg behavior in an IL containing the bis(trifluoromethanesulfonylimide) ([Tf₂N]) anion. The results show an irreversible deposition/dissolution of Mg at a high water concentration (ca. 1300 ppm, 50 mmol L⁻¹) and very low reversibility (7.3%) at a moderate water concentration (ca. 65 ppm, 5 mmol L⁻¹). The formation of a film on the electrode surface and the presence of Mg were confirmed by scanning electron microscopy and energy-dispersive X-ray spectroscopy (SEM-EDS). The process irreversibility indicates the formation of a passivating film. Because the presence of water affects the reversibility of the process, studies of Fe deposition/dissolution were conducted in two different ILs and with microelectrodes to evaluate how the water modifies the reversibility and the diffusion of ions. Water plays an important role in the reversibility of Fe deposition/dissolution being that deposition is less reversible when water is absent. The Fe diffusion is also modified because the Fe ion coordination sphere is strongly affected by the presence or absence of water; the Fe diffusion was also shown to depend on the coordination ability of the cation.

Keywords: passivation, water effect, reversibility, microelectrode, metal deposition, ionic liquids

Introduction

Over the past few years, ionic liquids (ILs) have attracted increasing attention as electrolytes in electrochemical devices such as Li-ion batteries,¹⁻⁵ supercapacitors⁶⁻¹⁰ and electrochromic devices.^{11,12} Because of their wide electrochemical window, the ILs are also promising electrolytes for the electrodeposition of metals and

alloys that, because of their highly negative reduction potential, cannot be deposited from aqueous or organic solutions.¹³⁻¹⁵ In addition, ILs are liquids and are stable over a wide temperature range, with upper temperature stability limits as high as 400 °C, at least for a short time. This stability enables electrodeposition to be conducted at various temperatures, allowing the electrodeposition of metals that are thermodynamically more favorable specific temperatures, as Tantalum.¹⁶ However, despite the high electrochemical stability of ILs, these electrolyte media are exclusively composed of ions that can coordinate with the

*e-mail: rtorresi@iq.usp.br

[†]Both authors have contributed equally to this paper.

reducing species and form passivating layers on the surface of the electrode.¹⁷⁻¹⁹ In addition, because of the high number of cations and anions available that can be combined to form an IL, the choice of the most appropriated electrolyte for deposition of a given species represents a challenge and warrants intensive study.

Among several metals and alloys that can be deposited/dissolved, Mg is of special interest due to the possibility of its use as anode in rechargeable Mg batteries,²⁰⁻²² which would be advantageous due to Mg being less expensive and more abundant than lithium. Some reports related to the use of Mg in Mg-air batteries with ILs used as the electrolyte have recently appeared in the literature.^{23,24}

To the best of our knowledge, the reversible deposition/dissolution of Mg in ILs has not been observed using IL and Mg²⁺ salt as Mg source. In fact, in a series of papers, the group of Prof Yang demonstrated the deposition/dissolution of Mg in an IL containing the [BF₄]⁻ anion, where they used Mg(CF₃SO₃)₂ salt as the Mg source.²⁵⁻²⁸ However, Cheek *et al.* claimed that the solution used in some of these works was not possible to reproduce,²⁹ and our group also experienced this problem. Cheek *et al.* further showed that the deposition/dissolution of Mg using an IL containing the CF₃SO₃⁻ anion and an IL containing the bis(trifluoromethanesulfonylimide) ([Tf₂N]⁻) anion was not possible.²⁹ In other study, Murase *et al.* showed the water effect in the Mg dissolution in an IL with quaternary-ammonium cation.³⁰

On the basis of these assumptions, in this contribution, we performed a series of voltammetry experiments to understand the reversibility of the Mg deposition/dissolution in ILs containing [Tf₂N]⁻. The effect of small amounts of water in the system was evaluated. For a better understanding of this process, we also studied the influence of the presence of water on the electrochemistry of Fe in IL-based electrolytes.

Experimental

Chemicals

1-butyl-2,3-dimethylimidazolium bis(trifluoromethylsulfonyl)imide ([BMMI][Tf₂N]⁻, Iolitec-Germany, 99%, ca. 50 ppm water) (Figure 1), *N*-*n*-butyl-*N*-methylpiperidinium bis(trifluoromethylsulfonyl)imide ([BMP][Tf₂N]⁻, Iolitec-Germany, 99%, ca. 50 ppm water) (Figure 1), 1,2-dimethylimidazole (Sigma-Aldrich, 98%), 2-bromoethyl ethyl ether (Sigma-Aldrich, 90%), bis(trifluoromethane)sulfonylimide (Sigma-Aldrich, > 95%), bis(trifluoromethane)sulfonylimide lithium salt (Sigma-Aldrich, > 99%), dichloromethane, THF, acetonitrile

(Labsynth, Brazil), anhydrous Mg sulfate, and powdered Fe (Labsynth, > 98%) were used as received. Acetylacetonone (Sigma-Aldrich, ≥ 99%) (ACAC) was open inside of an argon-filled glove box (MBraun-Germany, Labmaster 130) with moisture and oxygen levels below 1 ppm and used as received.

Preparation of [EtO(CH₂)₂MMI][Tf₂N]⁻ and Fe(Tf₂N)₂

[EtO(CH₂)₂MMI][Tf₂N]⁻ (Figure 1) was prepared according to a previously reported method.³¹ Fe(Tf₂N)₂ and Mg(Tf₂N)₂ were prepared according to a method derived from that of Yamagata *et al.*³² as follows: an aqueous solution of ca. 1 mol L⁻¹ HTf₂N was added to a round-bottom flask containing an excess of powdered Fe or Mg flakes, and the mixture was stirred at room temperature for 24 h. The excess metal was removed by filtration, and the water was evaporated until a slurry was obtained, which was placed under vacuum (< 20 mbar) at 80 °C for 3 days, which resulted in a white solid. The solid was characterized by thermogravimetric analysis (TGA, 2950 thermogravimetric analyzer, TA Instruments), differential scanning calorimetry (DSC, Q10 differential scanning calorimeter, TA Instruments), Fourier-transform infrared spectroscopy (FTIR, Bomem MB100), inductively coupled plasma-atomic emission spectrometry (ICP-AES) (Spectro Ciros CCD ICP-AES) and elemental analysis (Perkin-Elmer CHN 2400 elemental analyzer). The results showed that the formulas of the obtained materials are Fe(Tf₂N)₂·4H₂O and Mg(Tf₂N)₂·6H₂O.

The tetrahydrated iron salt was further dried under vacuum (< 20 mbar) at 120 °C to obtain a brownish solid. Analysis of this solid shows that it consists of anhydrous Fe(Tf₂N)₂, and it was used to prepare Fe(Tf₂N)₂/IL mixtures with lower water content. After the Mg(Tf₂N)₂·6H₂O/IL mixture (100 mmol L⁻¹ of Mg²⁺) was prepared, it was maintained at 80 °C under vacuum until the humidity decreased to ca. 70 ppm (5 mmol L⁻¹ of H₂O), which means that the Mg²⁺ concentration is 20 times higher than the H₂O concentration in the driest Mg²⁺/IL mixture.

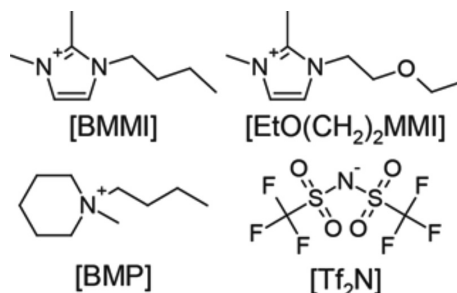


Figure 1. Structures of the ions that compose the ILs used in this work: [BMMI], [EtO(CH₂)₂MMI], [BMP] and [Tf₂N].

Electrochemical measurements

Platinum microelectrodes were fabricated from platinum fibers with different diameters (Roberplat-Brazil, 99%) according to the procedure previously described by Bertotti *et al.*³³ Microelectrodes with various radii were used as working electrodes (WE) in experiments involving Fe salts, with platinum wire used as a counter electrode (CE) and silver wire used as a *quasi*-reference electrode. In the case of Mg electrochemistry, a platinum macro electrode ($r = 0.8$ mm) was used as the WE and platinum mesh and wire were used as the CE and *quasi*-reference electrodes, respectively. All measurements were conducted in the glove box; the electrodes were connected to an Autolab PGSTAT30 potentiostat/galvanostat.

Scanning electron microscopy and energy-dispersive X-ray spectroscopy

Scanning electron micrographs were collected with a scanning electron microscope (SEM JSM-7401F, JEOL) coupled with an energy-dispersive spectrometer (EDX), an LEI detector, a 3.0 kV accelerating voltage and an 8 mm working distance were used. Specimens were prepared on Pt surfaces by chronoamperometry in a three-electrode cell similar to that used in the electrochemical experiments.

Results and Discussion

Magnesium electrochemistry in ILs

To study the electrochemical behavior of Mg in ILs, we determined the electrochemical window of the ILs [BMMI][Tf₂N] and [BMP][Tf₂N] using linear sweep voltammetry starting from open-circuit potential (OCP) and sweeping positive and negative potentials in two different experiments for each IL (Figure 2). The ILs exhibited similar positive limits (ca. 2.0 V vs. Ag); however, the negative limits varied. Whereas the IL with an imidazolium ([BMMI]) cation reached -1.25 V vs. Ag, the IL with piperidinium ([BMP]) cation reached -1.6 V vs. Ag. Therefore, we used the [BMP] cation in the study of the electrochemical behavior of Mg to enable experiments at more negative potentials. The choice of the anion ([Tf₂N]) was based on its chemical and electrochemical stability, its transport properties and the fact that this anion is widely used in studies concerning the use of ILs in energy storage devices.^{1,34}

Although Zhao *et al.* claimed that the deposition/dissolution of Mg using the anion [Tf₂N] cannot be achieved,³⁵ it is important to understand the electrochemical behavior of Mg in the ILs with [Tf₂N] anion.

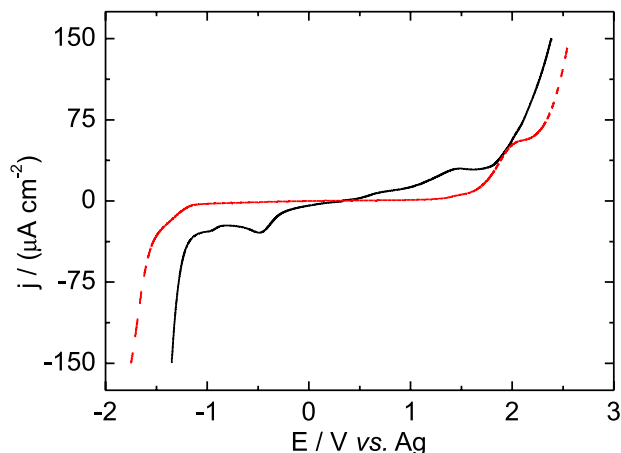


Figure 2. Linear voltammetry of the ILs [BMMI][Tf₂N] (solid black line) and [BMP][Tf₂N] (dashed red line) at 10 mV s⁻¹; the scans were started from OCP (0.33 V and 0.0 V vs. Ag for [BMMI][Tf₂N] and [BMP][Tf₂N], respectively) and were scanned in both directions (negative and positive potentials). WE and CE were platinum disk and mesh, respectively.

The voltammograms in Figure 3 show the effect of water concentration on the electrochemical behavior of the IL. A ten-fold increase in water concentration leads to a drastic modification of the cyclic voltammetry (CV) profile, where the cathodic process shifted to lower potentials, leading to a narrower electrochemical window for the electrolyte. In the reverse scan, an anodic peak is observed at ca. -2.0 V vs. Pt, which can be related to two phenomena: first, it may represent the oxidation of species generated from the IL degradation; second, it may represent the oxidation of the H₂ formed during the water reduction because the IL exhibits high viscosity and the H₂ should exhibit low diffusion from the electrode surface to the bulk. The other anodic peaks at higher potentials may be related to the IL degradation because they are not present in the linear sweep voltammograms shown in Figure 2.

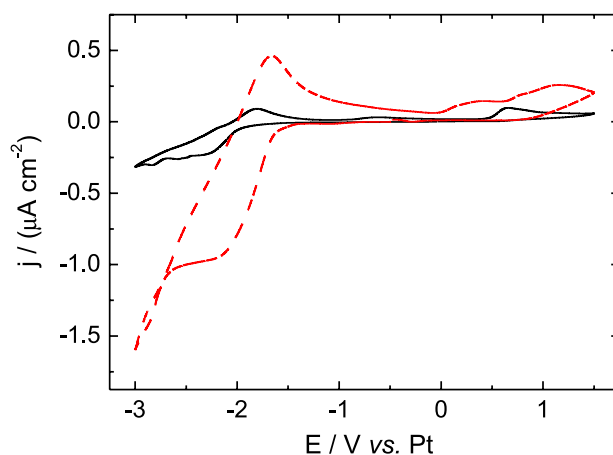


Figure 3. Cyclic voltammograms of [BMP][Tf₂N] with 5.0 mmol L⁻¹ (solid black line) and 50 mmol L⁻¹ (dashed red line) water at 10 mV s⁻¹. WE and CE were platinum disk and mesh, respectively.

The electrochemical behavior of Mg^{2+} was evaluated in a mixture of 100 mmol L^{-1} of $\text{Mg}(\text{Tf}_2\text{N})_2$ in $[\text{BMP}][\text{Tf}_2\text{N}]$. Figure 4a shows the CV of this solution with the lower water concentration (5 mmol L^{-1} , or 65 ppm). Upon first observation, no reduction of Mg^{2+} is apparent, and the cathodic current observed appears to be related to the IL degradation. However, some groups have reported that the addition of Li^+ salts stabilizes ILs with imidazolium cations and $[\text{Tf}_2\text{N}]$ and $[\text{BF}_4]$ anions, leading to a wider electrochemical window in the cathodic limit,³⁶⁻³⁹ this fact is also noticed when Mg^{2+} is added to the $[\text{BMP}][\text{Tf}_2\text{N}]$, as can be seen from Figure 3 and Figure 4a, and should enable the reduction of Mg^{2+} at a higher overpotential than that of the neat IL degradation. Moreover, the current loop (indicated by arrows in Figure 4a) in the reverse scan suggests that film formation occurs in the electrode surface driven by an overpotential nucleation/growth process.⁴⁰ Results that discuss the Mg^{2+} reduction will be addressed in the following paragraphs. Two anodic peaks related to film oxidation appear after the current loop; however, the very low coulombic relationship (7.3%) indicates that the deposition/dissolution is irreversible.

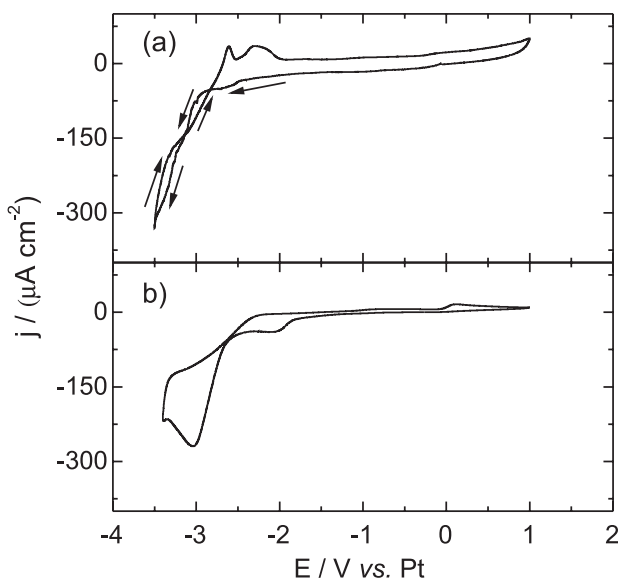


Figure 4. Cyclic voltammograms of 100 mmol L^{-1} $\text{Mg}(\text{Tf}_2\text{N})_2$ in $[\text{BMP}][\text{Tf}_2\text{N}]$ with 5 mmol L^{-1} (a) and 50 mmol L^{-1} (b) water at 10 mV s^{-1} . WE and CE were platinum disk and mesh, respectively.

Figure 4b shows the CV of 100 mmol L^{-1} $\text{Mg}(\text{Tf}_2\text{N})_2$ in $[\text{BMP}][\text{Tf}_2\text{N}]$ with the presence of 50 mmol L^{-1} water (1300 ppm). The cathodic process is shifted to less negative potentials, and a cathodic current -1.75 V vs. Pt is observed, that may be related to water reduction, before the concomitant reduction of water and Mg at more negative potential. The metal deposition is completely irreversible due to the lack of anodic current. The absence

of anodic current must be related to chemical oxidation and passivation of the film due to the increased water content.

Analyses of SEM and EDX spectroscopy were performed on a film obtained at constant potential (-3.0 V vs. Pt for 24 h in 100 mmol L^{-1} $\text{Mg}(\text{Tf}_2\text{N})_2$ in $[\text{BMP}][\text{Tf}_2\text{N}]$) to evaluate the film formation indicated by the CV profile of Figure 4a. A granular film above the Pt electrode is observed in the SEM image in Figure 5. EDX spectroscopy performed on the film in Figure 5 confirms the presence of Mg in the film; however, the presence of O is also observed, at this point, some proposes may be drawn. First, water reacts with Mg , leading to the formation of MgO ; it is also evident the superficial formation of MgO due to Mg oxidation in air during the SEM sample preparation. Second, the water reduction may occur instead of Mg reduction and lead to the $\text{Mg}(\text{OH})_2$ precipitation, considerations concerning these proposes will be made

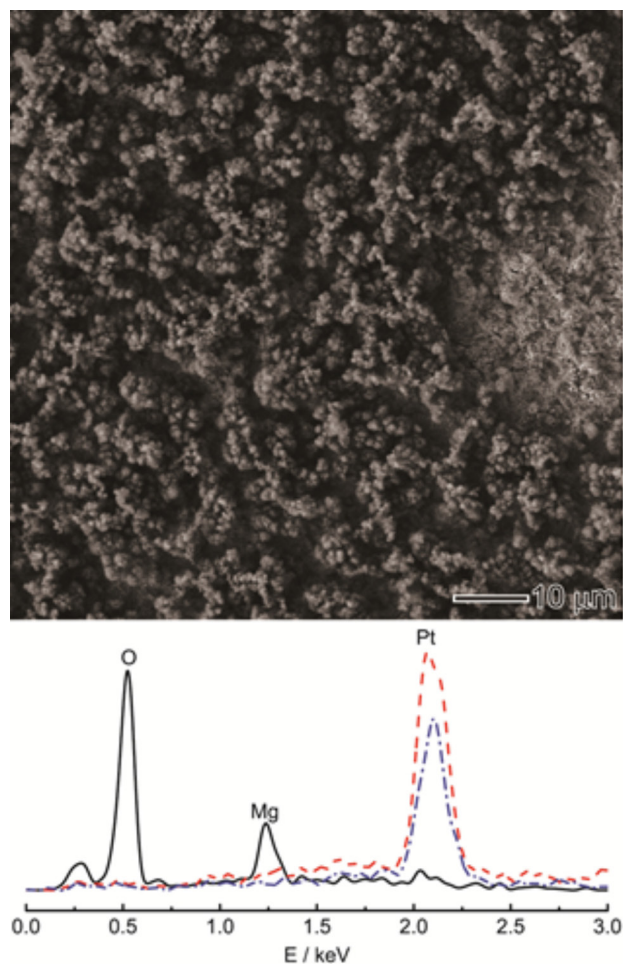


Figure 5. Scanning electron micrograph of a Mg film on a Pt electrode obtained from a chronoamperometry at -3.0 V vs. Pt for 24 h in 100 mmol L^{-1} $\text{Mg}(\text{Tf}_2\text{N})_2$ in $[\text{BMP}][\text{Tf}_2\text{N}]$. EDX spectra of the Mg film (black full line), a Pt electrode subjected to chronoamperometry at -3.0 V vs. Pt for 24 h in neat $[\text{BMP}][\text{Tf}_2\text{N}]$ (red dashed line) and a Pt electrode that remained at OCP in 100 mmol L^{-1} $\text{Mg}(\text{Tf}_2\text{N})_2$ in $[\text{BMP}][\text{Tf}_2\text{N}]$ for 24 h (blue dash-dotted line).

ahead. To evaluate the presence of Mg in the film, two more samples were prepared as control: one in which the Pt electrode was submitted to chronoamperometry (-3.0 V vs. Pt for 24 h) in neat [BMP][Tf₂N] and another in which the Pt electrode remained at OCP in the solution of 100 mmol L^{-1} Mg(Tf₂N)₂ in [BMP][Tf₂N] for 24 h. The EDX spectra of both electrodes show only the band related to Pt, confirming that the cathodic current in the voltammogram shown in Figure 4a is due to the formation of a film containing Mg.

To better understand the role of water during the cathodic process, one can consider the experiments performed by Cheek *et al.*,²⁹ concerning the Mg electrodeposition in mixture of Grignard reagent and IL in certain conditions. This is an interesting approach, since Grignard reagent reacts with water, guaranteeing a water-free electrolyte. They observed a CV profile with cathodic process and the absence of any anodic process, indicating that, even in a dry mixture, the Mg passivation is observed.

At this point, we conclude that the reduction of Mg²⁺ in [BMP][Tf₂N] is viable, although dissolution is not observed - at least not with high efficiency. Two hypotheses can explain the irreversibility of the deposition/dissolution. First, water is also reduced, resulting in the generation of OH⁻, and then Mg(OH)₂ precipitates on the deposited Mg, thereby causing its passivation. Second, the [Tf₂N] can also be reduced, resulting in the formation of other Mg²⁺ salts, such as Mg(SO₂CF₃)₂ and MgS₂O₄, which can also cause the Mg passivation; a similar process has been observed with Li.^{17,18}

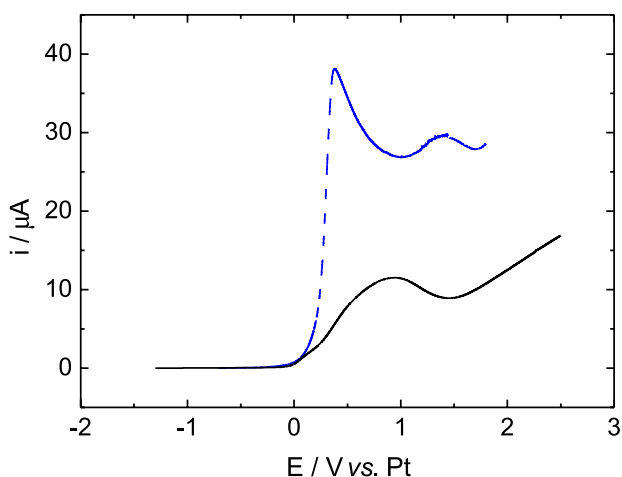


Figure 6. Linear voltammetry of Mg in neat [BMP][Tf₂N] (black solid line) and in a solution of 100 mmol L^{-1} acetylacetonate in [BMP][Tf₂N] at 1 mV s^{-1} starting at OCP. WE and CE were Mg ribbon and Pt mesh, respectively.

Lastly, the electrochemical behavior of metallic Mg was investigated in the [BMP][Tf₂N]. The linear voltammetry shown in Figure 6 starts at OCP in the anodic direction at

1 mV s^{-1} . No considerable current is observed until 0.0 V vs. Pt , when the anodic current increases and reaches a maximum. This result suggests a saturation of the electrode surface by Mg²⁺; afterwards, the current increases again. When 100 mmol L^{-1} ACAC is added to the IL, the voltammetric profile changes. ACAC is known to be a good coordinating compound for various metals, including Mg²⁺.⁴¹ The presence of ACAC in the IL shifts the anodic process to a lower potential (ca. -0.3 V vs. Pt) because it favorably alters the oxidation thermodynamics with respect to the neat IL. The Mg²⁺ solvation by ACAC removes these species from the electrode surface, and the anodic current reaches higher values.

Although the irreversibility of Mg deposition/dissolution in the [BMP][Tf₂N] is related to the passivation of the film by metal oxidation due to the presence of water or even due to the formation of salts generated by degradation of the anion, the use of a compound that exhibits strong coordinating properties has shown to be an interesting alternative to increasing the rate of Mg dissolution in an IL. This strategy could be applied in Mg batteries or related devices. Our results provide several hints to improving Mg deposition when working with IL electrolytes. In Figure 4, for example, the cathodic charge is 7% higher when the electrolyte is wet than when it is dry. This apparently small change is even more relevant when the changes in the deposition profile (i.e., the appearance of a current peak and the shift of deposition to less negative potentials) are considered; these changes indicate that the mechanism by which Mg²⁺ is being deposited has changed.

Iron electrochemistry in ILs

To better understand the electrochemical behavior of divalent metallic cations in IL media, voltammetric experiments on Fe(Tf₂N)₂·4H₂O in two different ILs (i.e., [BMMI][Tf₂N] and [EtO(CH₂)₂MMI][Tf₂N]) were conducted in the range of the Fe^{2+/0} pair. Because the deposition is a two-electron process, the results for Fe²⁺ and Mg²⁺ depositions can be compared. The cation of the ILs was also changed to assess the effect of a coordinating center (i.e., the oxygen in the ether functionality of [EtO(CH₂)₂MMI]), and the results were compared to those obtained in the absence of such a center (such as in the [BMMI] cation). Because Fe²⁺ deposits at lower cathodic potentials, the lesser electrochemical stability of the [BMMI] cations should not be problematic, especially because the anion, which has a greater influence on the deposition, was the same. The cyclic voltammograms of the Fe salt in both ILs using microelectrodes with different diameters are shown in Figure 7.

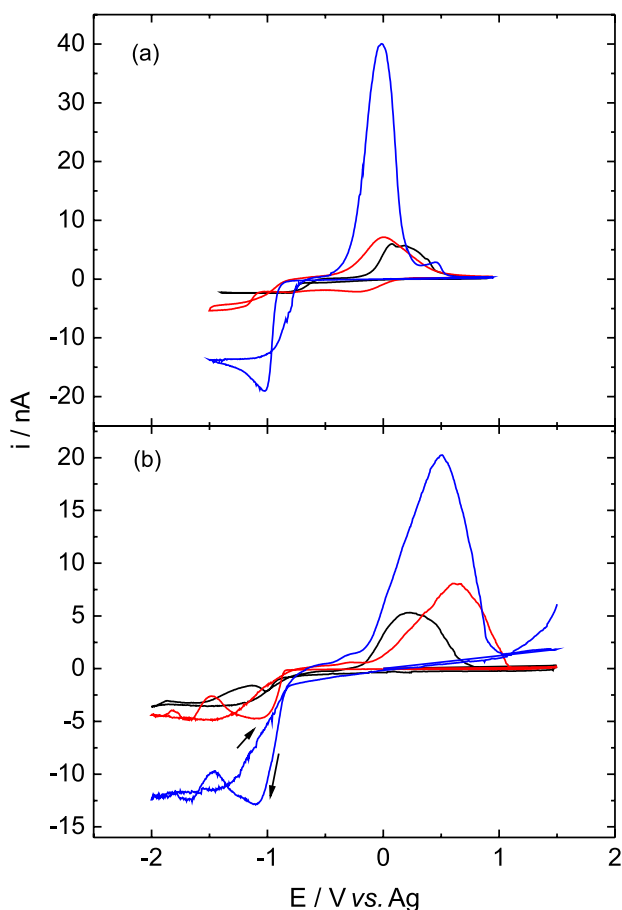


Figure 7. Voltammograms of $\text{Fe}(\text{Tf}_2\text{N})_2$ in $[\text{BMMI}][\text{Tf}_2\text{N}]$ (a) and $[\text{EtO}(\text{CH}_2)_2\text{MMI}][\text{Tf}_2\text{N}]$ (b) obtained using microelectrodes with radii of 11 (black), 24 (red) and 38 (blue) μm .

Deposition of metals in microelectrodes should have a mass transport regime that follows a hemispherical diffusion, as it is with normal electrochemistry in these electrodes, and, thus, a current plateau is expected.⁴² According to the results presented in Figure 7, deposition using the microelectrodes reaches a plateau-like regime at cathodic potentials, which indicates that, even in the highly viscous IL media, diffusion is primarily hemispherical, although somewhat hampered. The presence of a small peak in the voltammogram of the electrode with a radius of 38 μm also indicates that when the more viscous IL was employed ($[\text{BMMI}][\text{Tf}_2\text{N}]$ in Figure 7a), the electrode behavior starts approaching that of a macroelectrode. For clarity sake, the considered currents are indicated in Figures S1 and S2, in the Supplementary Information.

The diffusion coefficient of the Fe^{2+} species in the ILs can be determined from the plateau currents in Figure 7 because, according to equation 1, the plateau current is proportional to the electrode radius:

$$i_p = 4nFDCr \quad (1)$$

where i_p is the plateau current (A), n is the number of electrons involved, F is the Faraday constant ($96,485 \text{ C mol}^{-1}$), D is the diffusion coefficient ($\text{cm}^2 \text{ s}^{-1}$), C is the species concentration (mol cm^{-3}), and r is the electrode radius (cm). As expected, a linear correlation between the plateau current and the electrode radius was obtained with both ILs, as shown in Figure 8. Notably, in all of the previously discussed measurements, the concentration of the Fe salt was kept constant, thus avoiding any possible effect of its variation on the ILs' physico-chemical properties.

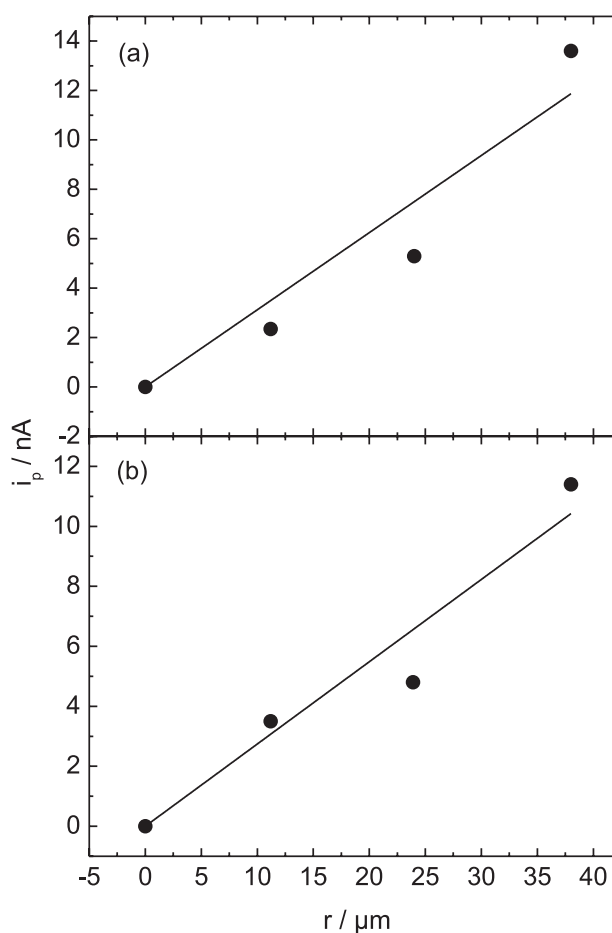


Figure 8. Plateau current vs. electrode radius for $\text{Fe}(\text{NTf}_2)_2$ in $[\text{BMMI}][\text{NTf}_2]$ (a) and $[\text{EtO}(\text{CH}_2)_2\text{MMI}][\text{NTf}_2]$ (b).

From Figure 8 and using equation 1, the diffusion coefficient in each medium can be determined. Notably, however, these values are for the case of wet mixtures; the water contents are summarized in Table 1. Also, the last point in Figure 8a deviates slightly from the observed tendency, in agreement with what was stated previously regarding the electrode exhibiting behavior that resembles that of a macroelectrode.

To observe the effect of water on the electrochemistry of Fe^{2+} in the IL media, the previously described mixtures

were also prepared after vacuum drying at 120 °C. After this process, we observed a dramatic change in the Fe salt, which was also observed after the mixtures were prepared; they acquired dark-red coloration, and apparently not all of the Fe salt added was promptly dissolved. However, the ICP analyses showed that the final concentration was the same as the analytical one. The results obtained after the drying process are presented in Figure 9 and Figure 10.

Similar to the results observed with the wet mixtures, those obtained with the dry mixtures show a linear correlation between the plateau current and the electrode radius. Table 1 summarizes the diffusion coefficient for each case as well as the water content.

The above results can be compared to those of Katayama *et al.*,³² who conducted an extensive study on various Fe complexes in an IL medium, and special attention is given to the fact that, depending on the coordination of the metallic center, i.e., depending on its radius, a different diffusion coefficient was measured. Specifically, an inverse relationship was observed. As such, we can conclude from Table 1 that Fe²⁺/IL mixtures with low water content show a larger radius (i.e., a smaller diffusion coefficient) for the

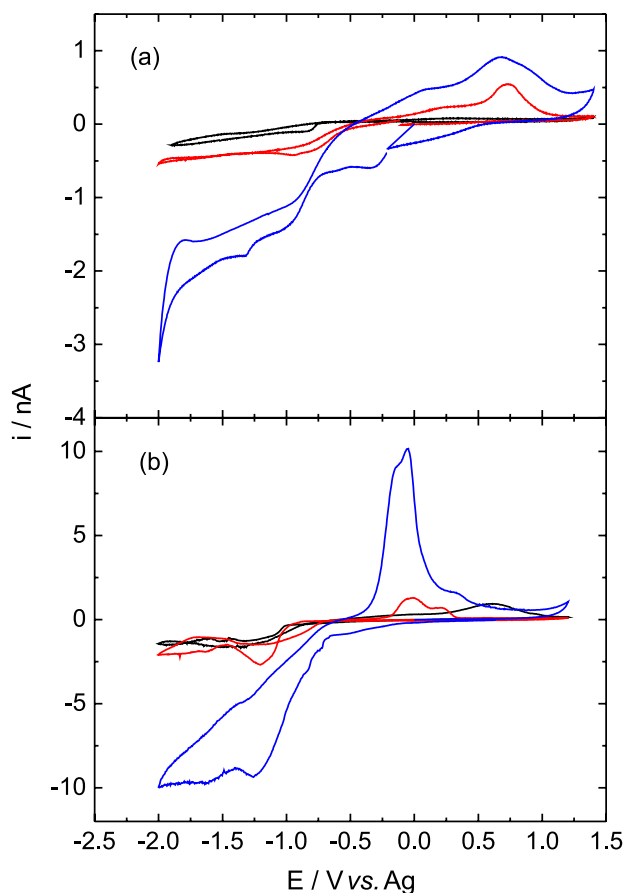


Figure 9. Voltammograms of Fe(Tf₂N)₂ in [BMMI][Tf₂N] (a) and [EtO(CH₂)₂MMI][Tf₂N] (b) after drying, with microelectrode radii of 8 (black), 11 (red) and 44 (blue) μm.

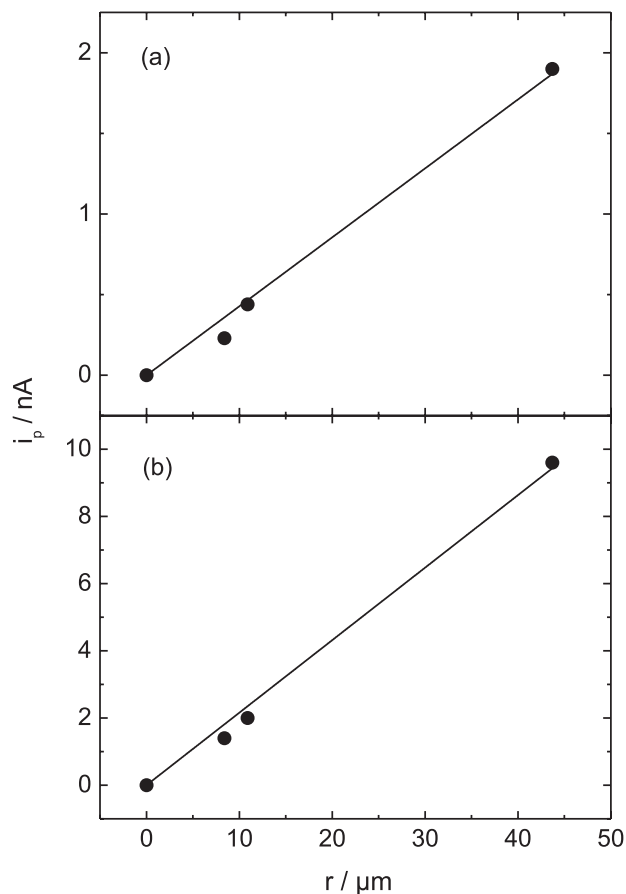


Figure 10. Plateau current vs. electrode radius for Fe(Tf₂N)₂ in [BMMI][Tf₂N] (a) and [EtO(CH₂)₂MMI][Tf₂N] (b) after drying.

Table 1. Diffusion coefficients and water contents of the IL/Fe(Tf₂N)₂ systems

IL	[H ₂ O] / ppm	D / (10 ⁻⁸ cm ² s ⁻¹)
[BMMI][Tf ₂ N]	1270	9 ± 1
	40	1.2 ± 0.1
[EtO(CH ₂) ₂ MMI][Tf ₂ N]	1570	7.9 ± 0.7
	110	6.2 ± 0.2

Fe complex, and the change is more pronounced in the case of the [BMMI] IL in comparison to the case of the [EtO(CH₂)₂MMI] IL. This difference can be attributed to the role water plays in coordinating Fe²⁺.

In the case of a wet mixture in [BMMI][Tf₂N], Fe²⁺ is mainly coordinated with water, which, in turn, leads to a smaller overall ionic radius. When the mixture is dry, Fe²⁺ is forced to coordinate with [Tf₂N] anions, which leads to a larger ionic radius. [EtO(CH₂)₂MMI][Tf₂N] mixtures are less sensitive to water removal, which is explained by the presence of a coordinating center in the cation: because the cation is also capable of coordinating Fe²⁺, water removal does not substantially change the coordinating sphere; thus, similar radii, i.e., similar diffusion coefficients, are measured.

The results in Figure S3 and Figure S4 in Supplementary Information show that the systems with higher water contents are significantly more reversible than the dry mixtures. These results, together with the observation of a color change and a smaller diffusion coefficient when water is removed, clearly indicate that the Fe^{2+} species coordinate differently depending on the water content. During electrodeposition of a metallic complex, the cation must lose some of its ligands to effectively reach the electrode surface;⁴³ by the same logic, it must acquire ligands to leave the electrode upon oxidation. In the case of $\text{Fe}^{2+}/\text{ILs}$, water can coordinate the oxidizing Fe^0 better than the $[\text{Tf}_2\text{N}]$ anion, which makes the oxidation of the deposited Fe easier (and consequently more reversible) in wet ILs in relation to its deposition in dry mixtures.

Notably, the previously discussed result does not disagree with the case of Mg (Figure 4) because of the difference in the passivation layers: if any passivation layer is present on the deposited Fe, its effect is negligible compared to the passivation layer on deposited Mg because Fe is deposited at less negative potentials than Mg, as stated previously. Thus, Mg deposition should be more reversible in the presence of a suitable coordination compound and sufficiently stable to not be reduced in the electrochemical window necessary to deposit Mg^{2+} . This requirement is also in agreement with the results presented in Figure 6, which show that, when ACAC is introduced to the IL, greater electrochemical dissolution of Mg^0 is observed, similar to the effect of the presence of water in Fe^{2+}/IL mixtures.

Conclusions

The electrodeposition of metallic cations in IL media is an attractive alternative to deposition in other solvents because of the intrinsic stability and safety of these electrolytes. Deposition in ILs is not without its own complications, however, such as the formation of a passivation layer and the high ionic force in the electrolyte. This high ionic force contributes to the formation of ionic pairs with the metallic cation of interest and can hamper deposition; furthermore, even highly stable electrolytes like ILs can still be attacked by the highly active Mg. However, these problems can be solved, and, as shown in this study, the presence of small additives, or even the introduction of an appropriate side chain into the cation of the IL, can strongly affect both the overall deposition rate and the reversibility of the deposition. As such, the advances presented here regarding the understanding of metallic deposition in IL media indicates which pathways to follow in the pursuit of increased viability of using

these novel electrolytes in Mg-based batteries; these approaches can also be extended to other metallic cations of interest.

Supplementary Information

Data concerning the Fe electrodeposition, as chosen current in plateau reduction (Figures S1 and S2) and the charge variation in function of potential (Figures S3 and S4) are available free of charge at <http://jbcbs.sbq.org.br>.

Acknowledgements

The authors acknowledge CNPq and FAPESP (09/53199-3) for financial support. LLC, TMB and VLM thank FAPESP (2011/16078-3, 2012/02117-0 and 09/09209-4, respectively) for the fellowships.

References

1. Armand, M.; Endres, F.; MacFarlane, D. R.; Ohno, H.; Scrosati, B.; *Nat. Mater.* **2009**, *8*, 621.
2. Benedetti, T. M.; Redston, E.; Menezes, W. G.; Reis, D. M.; Soares, J. F.; Zarbin, A. J. G.; Torresi, R. M. J.; *Power Sources* **2013**, *224*, 72.
3. Wongittharom, N.; Lee, T.-C.; Hsu, C.-H.; Ting-Kuo Fey, G.; Huang, K.-P.; Chang, J.-K.; *J. Power Sources* **2013**, *240*, 676.
4. Li, J.; Jeong, S.; Kloepsch, R.; Winter, M.; Passerini, S.; *J. Power Sources* **2013**, *239*, 490.
5. Chou, S.-L.; Wang, Y.-X.; Xu, J.; Wang, J.-Z.; Liu, H.-K.; Dou, S.-X.; *Electrochem. Commun.* **2013**, *31*, 35.
6. Benedetti, T. M.; Gonçalves, V. R.; Córdoba de Torresi, S. I.; Torresi, R. M.; *J. Power Sources* **2013**, *239*, 1.
7. Rennie, A. J. R.; Sanchez-Ramirez, N.; Torresi, R. M.; Hall, P. J.; *J. Phys. Chem. Lett.* **2013**, *4*, 2970.
8. Richey, F. W.; Dyatkin, B.; Gogotsi, Y.; Elabd, Y. A.; *J. Am. Chem. Soc.* **2013**, *135*, 12818.
9. Vatamanu, J.; Hu, Z.; Bedrov, D.; Perez, C.; Gogotsi, Y.; *J. Phys. Chem. Lett.* **2013**, *4*, 2829.
10. Kim, D.; Shin, G.; Kang, Y. J.; Kim, W.; Ha, J. S.; *ACS Nano* **2013**, *7*, 7975.
11. Desai, S.; Shepherd, R. L.; Innis, P. C.; Murphy, P.; Hall, C.; Fabretto, R.; Wallace, G. G.; *Electrochim. Acta* **2011**, *56*, 4408.
12. Zhou, D.; Zhou, R.; Chen, C.; Yee, W.-A.; Kong, J.; Ding, G.; Lu, X.; *J. Phys. Chem. B* **2013**, *117*, 7783.
13. Zein el-Abedin, S.; Endres, F.; *ChemPhysChem* **2006**, *7*, 58.
14. Endres, F.; Bukowski, M.; Hempelmann, R.; Natter, H.; *Angew. Chemie* **2003**, *42*, 3428.
15. Abbott, A. P.; McKenzie, K. J.; *Phys. Chem. Chem. Phys.* **2006**, *8*, 4265.
16. El Abedin, S. Z.; Endres, F.; *Acc. Chem. Res.* **2007**, *40*, 1106.

17. Howlett, P. C.; Brack, N.; Hollenkamp, A. F.; Forsyth, M.; MacFarlane, D. R.; *J. Electrochem. Soc.* **2006**, *153*, A595.
18. Zheng, J.; Gu, M.; Chen, H.; Meduri, P.; Engelhard, M. H.; Zhang, J.-G.; Liu, J.; Xiao, J.; *J. Mater. Chem. A* **2013**, *1*, 8464.
19. Martins, V. L.; Sanchez-Ramírez, N.; Calderon, J. A.; Torresi, R. M.; *J. Mater. Chem. A* **2013**, *1*, 14177.
20. Levi, E.; Gofer, Y.; Aurbach, D.; *Chem. Mater.* **2010**, *22*, 860.
21. Peng, B.; Liang, J.; Tao, Z.; Chen, J.; *J. Mater. Chem.* **2009**, *19*, 2877.
22. Aurbach, D.; Gofer, Y.; Lu, Z.; Schechter, A.; Chusid, O.; Gizbar, H.; Cohen, Y.; Ashkenazi, V.; Moshkovich, M.; Turgeman, R.; *J. Power Sources* **2001**, *97-98*, 28.
23. Khoo, T.; Somers, A.; Torriero, A. A. J.; MacFarlane, D. R.; Howlett, P. C.; Forsyth, M.; *Electrochim. Acta* **2013**, *87*, 701.
24. Khoo, T.; Howlett, P. C.; Tsaouria, M.; MacFarlane, D. R.; Forsyth, M.; *Electrochim. Acta* **2011**, *58*, 583.
25. Feng, Z.; NuLi, Y.; Wang, J.; Yang, J.; *J. Electrochem. Soc.* **2006**, *153*, C689.
26. NuLi, Y.; Yang, J.; Wang, J.; Xu, J.; Wang, P.; *Electrochem. Solid-State Lett.* **2005**, *8*, C166.
27. NuLi, Y.; Yang, J.; Wang, P.; *Appl. Surf. Sci.* **2006**, *252*, 8086.
28. NuLi, Y.; Yang, J.; Wu, R.; *Electrochem. Commun.* **2005**, *7*, 1105.
29. Cheek, G. T.; O'Grady, W. E.; El Abedin, S. Z.; Moustafa, E. M.; Endres, F.; *J. Electrochem. Soc.* **2008**, *155*, D91.
30. Murase, K.; Sasaki, I.; Kitada, A.; Uchimoto, Y.; Ichii, T.; Sugimura, H.; *J. Electrochem. Soc.* **2013**, *160*, D453.
31. Monteiro, M. J.; Camilo, F. F.; Ribeiro, M. C. C.; Torresi, R. M.; *J. Phys. Chem. B* **2010**, *114*, 12488.
32. Yamagata, M.; Tachikawa, N.; Katayama, Y.; Miura, T.; *Electrochim. Acta* **2007**, *52*, 3317.
33. Paixão, T. R. L. C.; Bertotti, M.; *Electrochem. Commun.* **2008**, *10*, 1180.
34. Zhao, L.; Yamaki, J.; Egashira, M.; *J. Power Sources* **2007**, *174*, 352.
35. Zhao, Q.; NuLi, Y.; Nasiman, T.; Yang, J.; Wang, J.; *Int. J. Electrochem.* **2012**, *2012*, 1.
36. Fuller, J.; Carlin, R. T.; Osteryoung, R. A.; *J. Electrochem. Soc.* **1997**, *144*, 3881.
37. Matsumoto, H.; Kageyama, H.; Miyazaki, Y.; *Electrochemistry* **2003**, *71*, 1058.
38. Fukuda, Y.; Tanaka, R.; Tshikawa, M.; *Electrochemistry* **2007**, *75*, 589.
39. Martins, V. L.; Nicolau, B. G.; Urahata, S. M.; Ribeiro, M. C. C.; Torresi, R. M.; *J. Phys. Chem. B* **2013**, *117*, 8782.
40. El Abedin, S. Z.; Pölleth, M.; Meiss, S. A.; Janek, J.; Endres, F.; *Green Chem.* **2007**, *9*, 549.
41. Kundu, D.; Roy, S. K.; *Analyst* **1993**, *118*, 905.
42. Ferapontova, E.; Terry, J.; Walton, A.; Mountford, C.; Crain, J.; Buck, A.; Dickinson, P.; Campbell, C.; Beattie, J.; Ghazal, P.; *Electrochem. Commun.* **2007**, *9*, 303.
43. Greef, R.; Peat, R.; Peter, L. M.; Pletcher, D.; Robinson, J. In *Instrumental Methods in Electrochemistry*; Ellis Hoewood Limited: Southampton, 1985.

Submitted: October 7, 2013

Published online: December 19, 2013

FAPESP has sponsored the publication of this article.